Evaluating the Interplay of Molecular Mechanisms in Tumor Microenvironment

Dr. Maya Kaminer, Dr. Yael Aharoni, Dr. Rachel Alon, Dr. David Cohen, Dr. Neta Zaslavsky, and Dr. Liron Ben-Baruch

University of Tel Aviv, Department of Biochemistry; Weizmann Institute of Science, Department of Immunology; Tel Aviv Sourasky Medical Center, Department of Cancer Research

Abstract

Cancer stem cells (CSC) form a specific population within tumor can be targeted. We have recently developed an NCAMthe tumor that has been shown to have self-renewal and targeted nanosized conjugate of paclitaxel bound to a biodedifferentiation properties, increased ability to migrate and gradable polyglutamic acid polymer. In this work, we examform metastases, and increased resistance to chemotherapy. ined the ability of the conjugate to inhibit Wilms tumor Consequently, even a small number of cells remaining after by targeting the NCAM-expressing CSCs. Results show that therapy can repopulate the tumor and cause recurrence of the the conjugate selectively depleted the CSC population of the disease. CSCs in Wilms tumor, a pediatric renal cancer, were tumors and effectively inhibited tumor growth without causpreviously shown to be characterized by neural cell adhesion ing toxicity. We propose that the NCAM-targeted conjugate molecule (NCAM) expression. Therefore, NCAM provides a could be an effective therapeutic for Wilms tumor. Mol Cancer specific biomarker through which the CSC population in this Ther; 16(11); 2462–72. 2017 AACR.

Introduction

Neural cell adhesion molecule, NCAM (CD56), an immunoglobulin superfamily cell adhesion molecule, is associated with an aggressive biological behavior, elevated expression of stem-cell markers, and increased metastatic capacity in several tumor types (1). In neuroblastoma, glioblastoma, melanoma, and some ovarian tumors, NCAM was found to be overexpressed in the entire cancer cell population (2, 3). Neuroblastoma tumors, for example, show high NCAM expression, which is frequently related to disease progression and inhibition of tumor cell adhesion to the endothelium (1). In other tumors, NCAM expression was found to be associated with poor prognosis (1, 3–8).

Wilms tumor (WT; nephroblastoma) is a type of cancer that initiates in the kidneys. It is the most common type of pediatric renal malignancy. The majority of WT are characterized by a triphasic histological pattern consisting of blastemal, stromal, and epithelial elements. A small subset of WT contains widespread anaplastic histology consisting of nuclear enlargement, and irregular mitotic cells, which are associated with increased relapse risk and are classified as unfavorable histology tumors. The absence of such anaplastic features categorizes these patients to having favorable histology WT, which represents the patient population analyzed in this study (9). The standard of care for children of any age has been laid out by two main strategies. Most children in Europe are treated with preoperative chemotherapy, according to the International Society of Pediatric Oncology- Renal Tumor Study Group (SIOP-RTSG). In North America, patients are treated with upfront surgery prior to administration of chemotherapy, as per the National Wilms Tumor Study/Children's Oncology Group (NWTS/COG) protocols (10). These approaches, which combine a wide variety of chemotherapy agents, have a similar overall survival of nearly 85%. Current treatment of WT principally centers around vincristine and actinomycin-D (to include doxorubicin for higher risk categories) for several months. In general, surgery is usually followed by multimodal adjuvant therapy that varies according to molecular biology and histology of the tumor. In cases of diffuse (widespread) anaplasia, WT patients are treated with more intense types of chemotherapy using the drugs etoposide, cyclophosphamide, and carboplatin, along with mesna in addition to the standard drugs vincristine and doxorubicin. However, none of these standard drugs is cell- or target-specific. As a result, many off-target effects may be encountered using these agents, which could be avoided with greater drug specificity. Therefore, there is a great medical need to develop new potent, selective, and safe drugs for WT patients that are not cured as well as patients who experience recurrence of disease and suffer from toxicity of current regimens. This motivation led to the rational design of our current study.

Our previous work has indicated that the human WT blastema, the undifferentiated component of the tumor, is locked in a renal progenitor state, overexpressing genes that characterize early renal development and nephron progenitors in the nephrogenic cortex of the developing kidney (11–14). Thisdifferentiationarrest is not complete so that mature lineages appear in the tumor at varying proportions, mimicking mesenchymal to epithelial transition (MET) that occurs in nephrogenesis (15, 16). NCAM marks the multipotent nephron stem cell population and its epithelial progeny that appear in fetal life during MET and nephrogenesis (15, 17,18).Following completion of nephrogenesisat 34thweek of human gestation, it is not expressed in the nephron neither postnatal nor during adulthood. Mouse models introducing gene mutations into renal lineage have confirmed human data linking a transformed early renal stem/progenitor cell to development of WT (19–21).

Cancer stem cells (CSC) are a population of cancer cells within the tumor that have similar characteristics to normal stem cells, specifically in their ability to self-renew and give rise to all cell lineages found in the tumor. Additional features of CSCs include increased ability to migrate and form metastases, and increased resistance to chemotherapy (22, 23). Consequently, even a small number of CSCs remaining after therapy can repopulate the tumor and cause recurrence of the disease (23). Our previous findings have indicated that WT CSC's self-renew, reside in the tumor blastema, share features with multipotent nephron progenitors, and are plastic, e.g., differentiating to epithelial lineage in transplantation assays but also being able to transit towards earlier mesenchymal lineage (12, 15, 17, 24). What allows the isolation of these cells from the WT blastema is the expression of NCAM and ALDH1 (12, 17, 24). Hence, specific targeting of NCAM in the tumor has the potential to eliminate a cell population containing the CSCs responsible for propagation and recurrence of the tumor (14). Accordingly, it was shown that an NCAM-targeting antibody conjugate (IMGN901, lorvotuzumab

mertansine) led to tumor eradication in a human WT xenograft model (17). Studies with IMGN901 conducted by the Pediatric Preclinical Testing Program on WT xenografts confirmed these results (25). These studies have sparked clinical trials with lorvotuzumab mertansine for relapsing WT (https://clinicaltrials.gov/ct2/show/NCT02420873). However, there exists a need for newer and safer NCAM targeting compounds, especially as CSCs have been characterized by the expression of NCAM in other cancers as well, including hepatocellular carcinoma, hepatoblastoma and pleuropulmonary blastoma, indicating it may serve as a broader therapeutic target (26, 27).

Here, we hypothesized that an NCAM-targeted polymer drug conjugate can be used to target both tumors with high NCAM expression as well as NCAM-CSC populations within tumors and the tumor blood vessels. An attractive polymeric carrier, which uses NCAM as a selective target for drug delivery to the tumor, should be water-soluble, nontoxic and multivalent such as polyglutamic acid (PGA; refs. 28–30). The polymeric backbone is composed of units of naturally occurring L-glutamic acid linked together through amide bonds. The pendant free g-carboxyl groups in each repeating unit are negatively charged at a neutral pH, which renders the polymer water-soluble, they also provide functionality for drug attachment. PGA is enzymatically biodegradable by cathepsin B, highly expressed in most tumor tissues (31–34). Moreover, it is nonimmunogenic and enables multivalent binding of drugs as well as targeting moieties. Hence, when used at an appropriate nanoscaled size, PGA conjugate can allow selective extravasation-dependent delivery to tumors via leaky angiogenic tumor vessels (29, 35, 36).

Several study cases report dramatic and favorable responses of WT patients to the tubulin inhibitor, paclitaxel (PTX), in addition to the more commonly used vincristine (37–39). Therefore, we selected to use PTX in this study for which the chemical reaction required for binding it to a polyglutamic acid nanocarrier is relatively simple and elegant as we reported previously (35, 36). To that end, this approach is attractive from the translational clinical point of view. We have previously developed an NCAM-targeted-peptide (NTP) conjugate of PGA with PTX named here PGA–PTX–NTP conjugate. This conjugate effectively inhibited the growth of neuroblastoma, a high NCAM-expressing tumor in mice, and did not have the toxic side effects associated with free PTX such as weight loss, decreased WBC count and neurotoxicity (36). Our goal in this work was to determine the ability of PGA–PTX–NTP to inhibit WT by targeting the NCAMexpressing CSCs.

Materials and Methods

Ethics statement

All animal procedures were performed in compliance with Tel Aviv University and Sheba Medical Center guidelines approved by the Institutional Animal Care and Use Committees (IACUC).

NCAM targeting peptide (NTP) synthesis

Two known peptides (40) were synthesized using solid phase peptide synthesis (SPPS) method on Sieber amide resin: (i) an NCAM targeting peptide with the sequence ASKKPKRNIKA (NTP) and (ii) a control peptide with the sequence ASKKPAANIKA (cNTP). Glycine was added at the N-terminal as a linker to allow conjugation to the PGA as previously described (36).

Synthesis of PGA–PTX–NTP

The conjugate was synthesized as described in refs. (35, 36). Briefly, the NCAM-targeting peptide and PTX were conjugated to PGA by carbodiimide coupling. The conjugate was treated with $NaHCO_3$ to transform it into the sodium salt, water-soluble form, and purified on a size exclusion chromatography column.

Cell culture

Isolation of Wilms tumor cells. To achieve single-cell suspensions, tumor samples were first dissolved by mincing them in Iscove's Modified Dulbecco's Medium (IMDM) supplemented with 1% penicillin–streptomycin (pen-strep) 100 mol/L (Biological Industries), and soaked in collagenase type IV (Sigma-Aldrich) for 1 hour at 37C. Next, the digested tissues were gradually forced through 100 mm and 70 mm cell strainers to achieve single-cell suspension. After removal of the digestion medium, cells were washed in red blood cells (RBC) lysis solution (comprised of 8.3 g NH_4Cl, 1.0 g $KHCO_3$, 1.8 mL of 5% EDTA in double distilled H_2O) at 1 mL/5 mL cell suspension ratio for 2 minutes at 4C. Cells were then resuspended in IMDM growth medium supplemented with 10% fetal bovine serum (Invitrogen), 1% pen-strep 100 mol/L, 1% L-glutamine (both from Biological Industries), 50 ng/mL epidermal growth factor (EGF), 50 ng/mL basic fibroblast growth factor (bFGF) and 5 ng/mL stem cell factor (SCF; all growth factors were purchased from PeproTech Asia).

For this study, two patient derived xenografts (PDX) lines were established out of two separate WT patients, from Sheba Medical Center, Tel Hashomer, and propagated in mice for five generations. These xenograft lines were generated from favorable histology WT. They were expanded in vivo to achieve more blastema predominance (expansion of blastema at the expense of differentiated elements). Importantly, WT with blastemal predominance (after preoperative chemotherapy) is regarded as high-risk tumors and require more aggressive treatment (41). These xenograft lines were termed W011 and W038 and were used for the in vitro and in vivo experiments at the fifth course of propagation. W011 cells were isolated in 2008 from a recurrent Wilms tumor of a 7-year-old female originally bearing a Triphasic-Blastemal predominance favorable histology tumor that showed features of local anaplasia. Its loss of heterozygosity (LOH) status 1p/16q was not known. The recurrence indicates a more aggressive treatment-resistant form of disease. W038 cells were isolated in 2013 from a primary tumor resected from a 5-year-old male bearing a Triphasic-Blastemal predominance with favorable histology tumor, treated using COG protocol and with a negative LOH status. When used in vitro, the patient-derived cells were plated after suspension and used immediately for the relevant assays; therefore, it was irrelevant to test for mycoplasma contamination.

Cellproliferation assay. Cells were plated onto 24-well plates (3

10^4 WT cells/well) and allowed to attach for 24 hours. Cells were incubated with the conjugates and free drugs, dissolved in cell culture medium at serial concentrations, for 72 hours. PTX treatment concentrations ranged from 0.01 to 10,000 nmol/L, according to PTX-equivalent concentration. PGA was used at concentrations equivalent to the PGA content in PGA-PTX or PGA-PTX-NTP conjugate. Following incubation, cells were washed, detached by trypsin, and counted by Coulter Counter (Beckman Coulter). Each experiment included at least 3 replicates and was repeated 3 times.

Migration (scratch) assay. The migration of cancer cells in the presence of conjugates and controls was evaluated using the scratch

assay. A scratch was done on a confluent cell monolayer using a tip, and cells were incubated with the conjugates and the free drugs at PTX-equivalent concentration of 100 nmol/L for 24 hours. Plates were imaged and the gap width was measured at the beginning and end of the experiment, at the same reference points. Each experiment included at least 3 replicates and was repeated 3 times.

Evaluation of the antitumor activity of the conjugate and its toxicity in a patient-derived Wilms tumor model in mice

Tumors were established in NOD/SCID mice from a single primary tumor that was propagated in mice for five passages (W038 xn5). The tumor was enzymatically dissociated into single-cell suspension and 1 10^6 cells in 100 mL 1:1 serum free medium/Matrigel (BD Biosciences) were injected subcutaneously into the left lower flank of NOD/SCID mice. Mice bearing palpable xenografts were randomized prior to treatment initiation. Five weeks after tumor inoculation, mice were treated intravenously (i.v.) with conjugates (PGA-PTX-NTP (n ¼ 5), PGA-PTX-cNTP (n ¼ 4), PGA-PTX (n ¼ 6), free PTX (n ¼ 5), and saline (n ¼ 4)). Mice were treated every other day, five treatments in total. All treatments were administered at 15 mg/kg PTX equivalent dose. Tumors were measured by a digital caliper and tumor volume was calculated as follows: width^2 length 0.52. Body weight and tumor size were monitored every other day. Two days after the last treatment, mice were euthanized and tumors were measured. NCAM expression in tumors treated with PGA-PTX-NTP was measured before, after three treatments, and after four treatments (tumors were taken for analysis at each time point).

Flow cytometry

Freshly removed patient-derived tumors (Xns) were dissociated into a single-cell suspension as described above and immediately analyzed. Cells were suspended in FACS buffer consisting of 0.5% BSA (Sigma-Aldrich) and 2 mmol/L EDTA (Biological Industries) in Dulbecco's Phosphate Buffered Saline (PBS; Biological Industries), and blocked with a mixture of FcR blocking reagent (MiltenyiBiotec) and human serum (1:1). For NCAM (eBiosience, 1205942) labeling, cells were incubated with the antibody at a concentration of 5 mg antibody per 10^6 cells for 30 minutes, in the dark, at 4C. Cell viability was tested using 7-amino-actinomycinD (7AAD) viability staining solution (eBioscience). Cell labeling was detected using FACS Calibur (BD Pharmingen). FACS results were analyzed using FlowJo analysis software. Viable cells were defined by their Forward Scatter/Side Scatter (FSC/SSC) profiles and lack of 7AAD staining. All quantitative measurements were made in comparison with the antibody IgG isotype (eBioscience).

Histology

H&E, caspase 3, Ki-67, and Pax8 histological staining were performed on formalin-fixed paraffin-embedded tumors. Staining was done with Caspase-3 (CP 229 A) mouse monoclonal IgG primary antibody (Biocare Medical) for apoptosis, Rabbit antiKi-67 (RBK027-05, Zytomed) for proliferation, Pax8 was stained using mouse monoclonal antibody (Cell Marque), anti-human CD56 primary antibody for NCAM (CD56; BioLegend), and mouse anti-ALDH for Aldehyde dehydrogenase 1 (ALDH1) staining (BD Biosciences) as was previously described (24, 36). All were followed by Histostain Broad spectrum kit (Invitrogen) and Liquid DAB substrate kit (Invitrogen).

Statistical methods

In vitro assays data were expressed as mean SD and in vivo experiments as SEM. Statistical significance was determined using an analysis of variance (ANOVA).

Results

PGA–PTX–NTP conjugate

A PGA-based conjugate bearing PTX and NTP (PGA–PTX–NTP) and control conjugates (PGA–PTX–cNTP and PGA–PTX) were synthesized and characterized. Structure of the conjugate is depicted in Fig. 1. Physico-chemical characterization results were described previously (36).

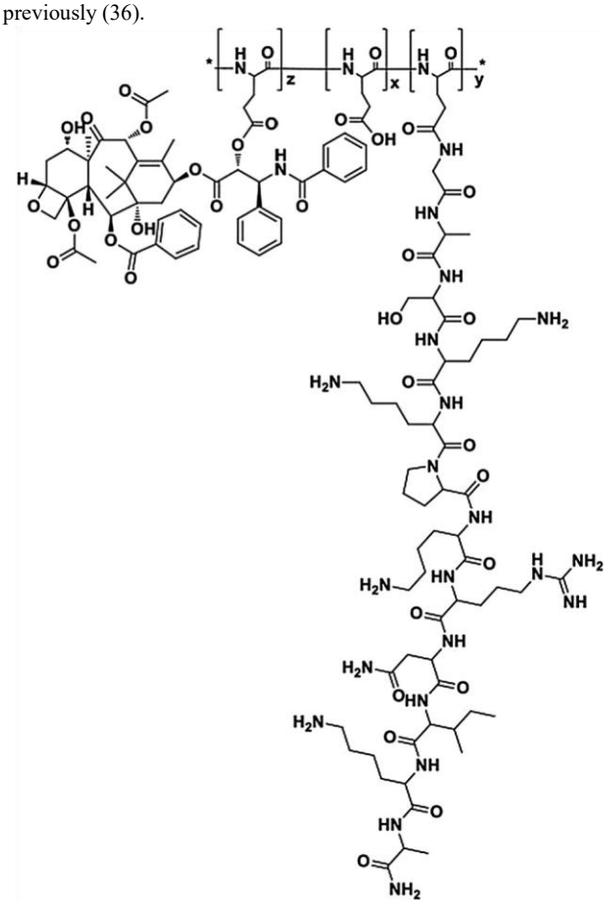

Figure 1.
Structure of the PGA–PTX–NTP conjugate.

Evaluation of the cytotoxic effect of PGA–PTX–NTP conjugate on Wilms tumor cells

The conjugate's activity was evaluated in vitro on proliferation of WT cells isolated from two patient-derived tumors, W038 xn5 and W011 xn4. Prior to evaluation of the antiproliferative effect of the conjugates, we determined the presence of an NCAM-expressing

population fraction. Both patient-derived cells expressed high levels of NCAM (Fig. 2).

Cells were incubated with the conjugates (PGA–PTX–NTP, PGA–PTX–cNTP, PGA–PTX), free PTX and PGA for 72 hours. PGA–PTX–NTP had a high cytotoxic activity on both patientderived WT cell cultures, showing that the drugs are released from the polymer and retaintheir activity. PGA–PTX–NTP inhibited the proliferation of WT cells at a slightly lower, yet significant, IC_{50} value compared with control PGA–PTX–cNTP conjugate and nontargeted PGA–PTX. The similar IC_{50} values at the same order of magnitude suggest that the PTX release from all conjugates retained its antiproliferative (tubulin inhibitory) activity. PGA had no cytotoxic effect in all the concentrations examined (Fig. 3A and B). IC_{50} values of the compounds are summarized in Table 1.

Evaluation of the effect of the PGA–PTX–NTP conjugate on patient-derived WT cells' migration

The migration of patient-derived WT cells in the presence of the PGA–PTX–NTP conjugate was evaluated using the scratch assay. A scratch was done on a 90% confluent cell monolayer, and cells were incubated with the conjugates and the free drug at PTXequivalent concentration of 100 nmol/L for 24 hours. Plates were imaged, and gap width was measured at the beginning and end of the experiment. PGA–PTX–NTP significantly inhibited the migration of the cells (Fig. 3C).

Wilms tumor an in vivo model

In W038 cells, the fraction of NCAM-expressing cells in the tumor decreased dramatically following treatments with PGA–PTX–NTP: from over 90% before treatment initiation, to 7% after only 3 treatments as measured by flow cytometry (Fig. 4A). Moreover, FACS analysis of cells that were suspended from all treated-groups' tumors at the endpoint of the study revealed that PGA–PTX–NTP treatment markedly decreased NCAM expression compared with the other treatments. NCAM expression at the end point was: Saline, 51%; PGA-PTX, 40%; PGA–PTX–cNTP, 62.5%; PGA–PTX–NTP, 8.9% (Fig. 4B). It can be seen that there was a marked reduction in NCAM expression, from 90% to 50%, even in the saline-treated group due to tumor progression and differentiation to a more epithelial phenotype, which expresses less NCAM. The acceptable differences between the NCAM levels amongst the mice treated with PGA–PTX–NTP (Fig. 4A and B, showing 0.29% and 8.97%, respectively) result from an anticipated biological variability between tumors' response to treatments and yet shows a marked decrease from control groups. NCAM-targeted PGA–PTX–NTP conjugate inhibited W038 tumor growth more than the control PGA–PTX–cNTP conjugate and the nontargeted PGA–PTX conjugate and was able to reduce the tumor size. Free PTX exhibited higher reduction of tumor size; however, mice in the PTX-treated group suffered from toxic side effects and significant weight loss following treatments (Fig. 5). This implies that the elimination of NCAM-expressing cells from the tumors can account for not only growth inhibition but also tumor volume reduction observed in three of the five PGA–PTX– NTP-treated tumors (Fig.5C). Obviously, PTX causedreduction in all surviving treated mice; however, this treatment was generally toxic and it can be seen that at the time of the acquired data, only 3 mice were left in the PTX-treated group which also suffered from severe weight loss (therefore euthanized).

Histology

H&E staining of tumors shows similar histology characteristics in the different treated groups. Xenografts are composed of mainly blastemal cells, while PGA–PTX–NTP tumors are devoid of differentiated elements. Ki-67 staining shows complete absence of proliferation in PGA–PTX–NTP-treated tumors, while in all other treatment groups there is substantial proliferation. Caspase-3 staining shows extensive apoptosis in tumors treated with free PTX, PGA–PTX–NTP and PGA–PTX. In tumors treated with PGA–PTX–NTP, apoptosis is seen in the core of the tumors, while in PGA–PTX–treated tumors, apoptosis is only seen at the margins. NCAM (CD56) staining was positive in mice treated with saline, while treatment with PGA–PTX and PGA–PTX–cNTP resulted in few cells stained for NCAM and treatment with PGA–PTX–NTP displayed no positive NCAM staining. This is in agreement with our conclusion from previous experiments that the targeted conjugate depletes NCAM-expressing cells. Aldehyde dehydrogenase 1 (ALDH1) staining shows positive staining in all treatments except of PGA–PTX–NTP, suggesting that the conjugate eliminated the CSC population defined

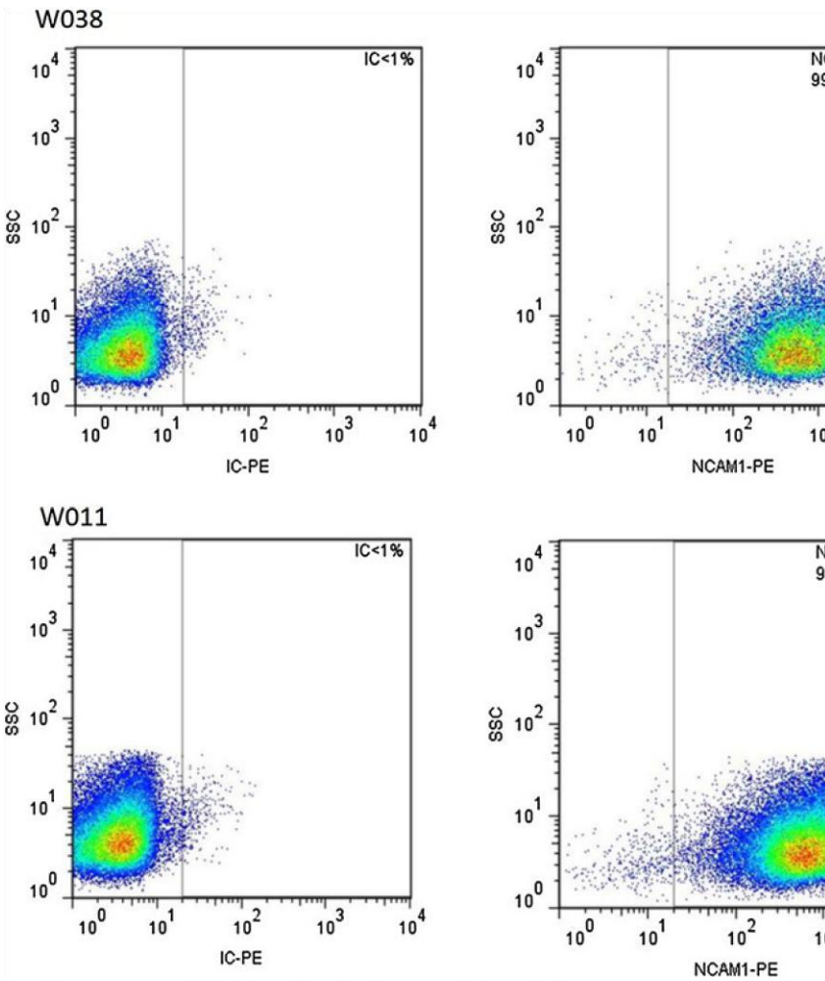

in this tumor as NCAMᵖ cells. Pax8, a nephric cell-lineage transcription factor, staining was positive in tumors from all the control groups, while in the PGA–PTX–NTP- treated group, very few cells were positively stained, suggesting that almost all NCAMᵖ cells were targeted and eliminated by the conjugate, leaving no epithelial cells in the lesion (Fig. 6).

Discussion

Several antibody-based systems for NCAM targeting were previously developed (42), among them humanized anti-NCAM antibodies (43–45), radioimmunoconjugates, and immunotoxins (46–51). To date, the most advanced NCAM-targeting therapeutic is huN901-DM1 (IMGN901), a humanized antibody conjugated to the cytotoxic drug maytansine (ImmunoGenInc). However, failure to achieve a sufficient improvement over current therapy (etoposide/carboplatin) using IMGN901 in a phase II clinical trial for small-cell lung carcinoma treatment resulted in a discontinuation of the trial in 2013.

We have successfully synthesized and characterized a novel conjugate that consists of an NCAM-targeting peptide (NTP) and paclitaxel (PTX) bound to the biodegradable PGA polymer (36). NTP is bound to PGA via a noncleavable amide bond, while PTX is bound via an ester bond that can be hydrolyzed by esterases in acidic pH. The peptide loading was 1.5 mol% in both PGA–PTX– NTP and PGA–PTX–cNTP, and drug loading was 7.5 mol% and 11 mol%, respectively, allowing a reliable comparison between the two conjugates. The conjugates' (with peptides) hydrodynamic radius was 10 nm, whereas of PGA-PTX was 5 nm. We predicted that 10 nm size would be sufficient to achieve selective accumulation via the enhanced permeability and retention (EPR) effect, while 5 nm size is at the lower range.

PGA–PTX–NTP had a strong cytotoxic activity on all patientderived WT cell cultures, showing that the drug is released from the polymer and retains its activity. PGA–PTX–NTP inhibited the proliferation of WT cells at a higher extent than the control PGA–PTX–cNTP conjugate and the nontargeted PGA–PTX, suggesting a faster and more efficient internalization of the NCAM-targeted conjugate. The free drug was more active than the conjugated one, because it rapidly crosses the cell membrane by diffusion. As expected, the advantage of the conjugate over the free drug was seen in vivo in terms of activity and safety.

NCAM-targeted conjugate exhibited enhanced antitumor activity compared with control PGA–PTX–cNTP conjugate on mice bearing a human WT patient-derived xenograft (PDX). We speculate that due to the preferential binding to NCAM-expressing cells, the targeted

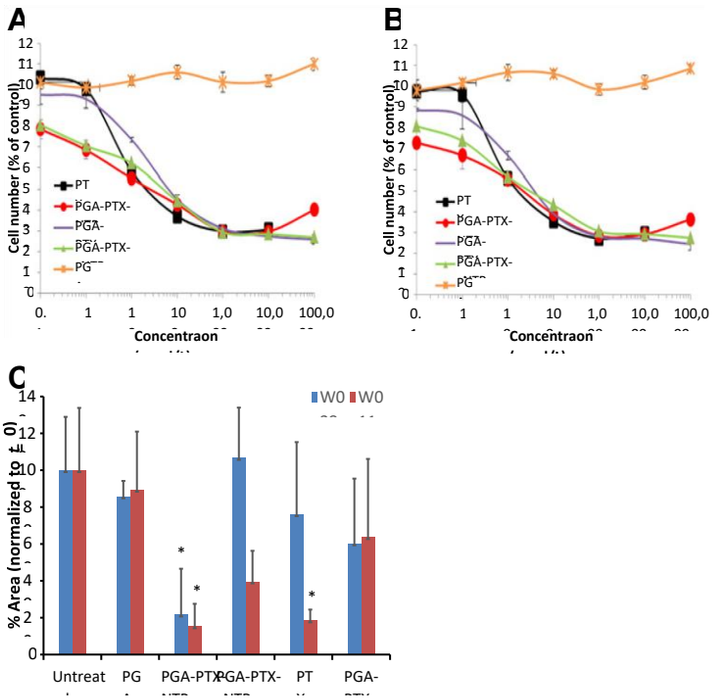

Figure 3.

PGA–PTX–NTP inhibited proliferation (A and B) and migration (C) of patient-derived WT cells. PGA had no cyto
24 hours of incubation, PGA–PTX–NTP showed significant inhibition of patient-derived WT cells' migration, at 1
closure was measured relative to time zero (C). , P< 0.05.

conjugate was able to accumulate and internalize more efficiently into tumor cells and their supporting tumor endothelial cells. This speculation is based on the current data and on previous data showing that the targeted conjugate, PGA–PTX–NTP, internalized preferentially and more rapidly to NCAM-expressing cancer cells as shown by FACS, and to endothelial cells as shown by inhibition of capillary-like tube formation compared with the nontargeted conjugate PGA–PTX–cNTP (36). PGA–PTX did not exhibit any activity, perhaps due to its small hydrodynamic size that did not allow for effective accumulation in the tumor.

Free PTX displayed increased activity; however, it was much more toxic, as evidenced by the high weight loss, as well as toxic deaths and WBC count decrease that was previously published (36). Therefore, while the free drug was already given at the maximum tolerated dose (MTD), we hypothesized that the dose of the conjugate can be increased further to improve its activity. Mice that were treated with saline and conjugates suffered some

Table 1. IC_{50} values of PGA–PTX–NTP conjugate and controls (nmol/L)

Cells treatment	W038 (IC_{50} nmol/L)	W011 (IC_{50} nmol/L)

PTX	20[1]	15[b]
PGA–PTX	60	40
PGA–PTX–cNTP	50	30[c]
PGA–PTX–NTP	20[a]	20[b]
PGA	NA	NA

weight loss as well; however, this weight loss can be attributed to the tumor's effect, as in this experiment, the treatments were initiated when the tumors were already very large (4 weeks after tumor inoculation) as clinically, Wilms tumors often become quite large before they are noticed. Therefore, this study design represents more realistically the clinical settings for a "regression trial" as opposed to a design representing a "prevention trial." In an additional experiment on a different cancer type (neuroblastoma), treatments were initiated at an earlier time point when tumors were smaller. In that experiment, PGA–PTX–NTP was compared with PGA–PTX–cNTP and PGA–PTX at 10 mg/kg PTX-equivalent dose, for 5 treatments q.o.d. (total dose of 50 mg/kg), and, additionally, given at 30 mg/kg (total dose of 150 mg/kg; ref. 36). The results confirmed that the NCAMtargeted conjugate is more effective than control PGA–PTX–cNTP and nontargeted PGA–PTX conjugates. Moreover, these results clearly demonstrate that the conjugate's dose can be significantly increased to obtain enhanced activity without aggravating toxicity, while free PTX cannot be given at a dose over 15 mg/kg at this dosing schedule. The complete absence of toxic effects for the PGA–PTX–NTP, i.e., weight loss,decrease in WBC count, and toxic death, suggests that the dose can be increased even further.

NCAM can also be exploited to target the tumor vasculature. We have previously shown that NCAM is expressed on human umbilical vein endothelial cells (HUVEC) during the process of capillary-like tube formation, but not in HUVEC cultured in
regular conditions (36). These results are in line with the work of Bussolati and colleagues, which showed that normal endothelial cells transiently acquired NCAM when organized in vessel-like

[1] P< 0.001 compared with PGA-PTX using ANOVA. [b]P¼ 0.017. [c]P¼ 0.022.

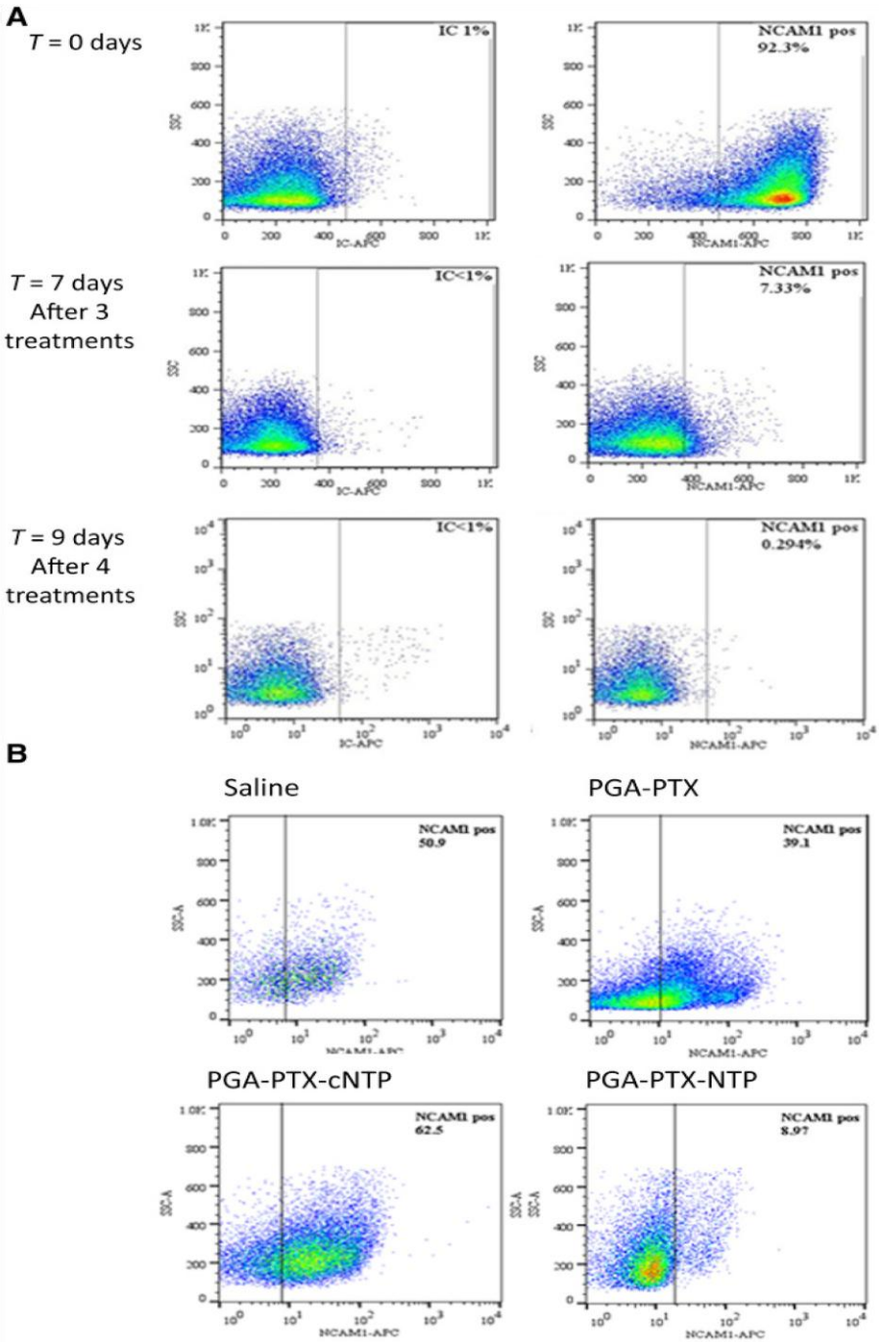

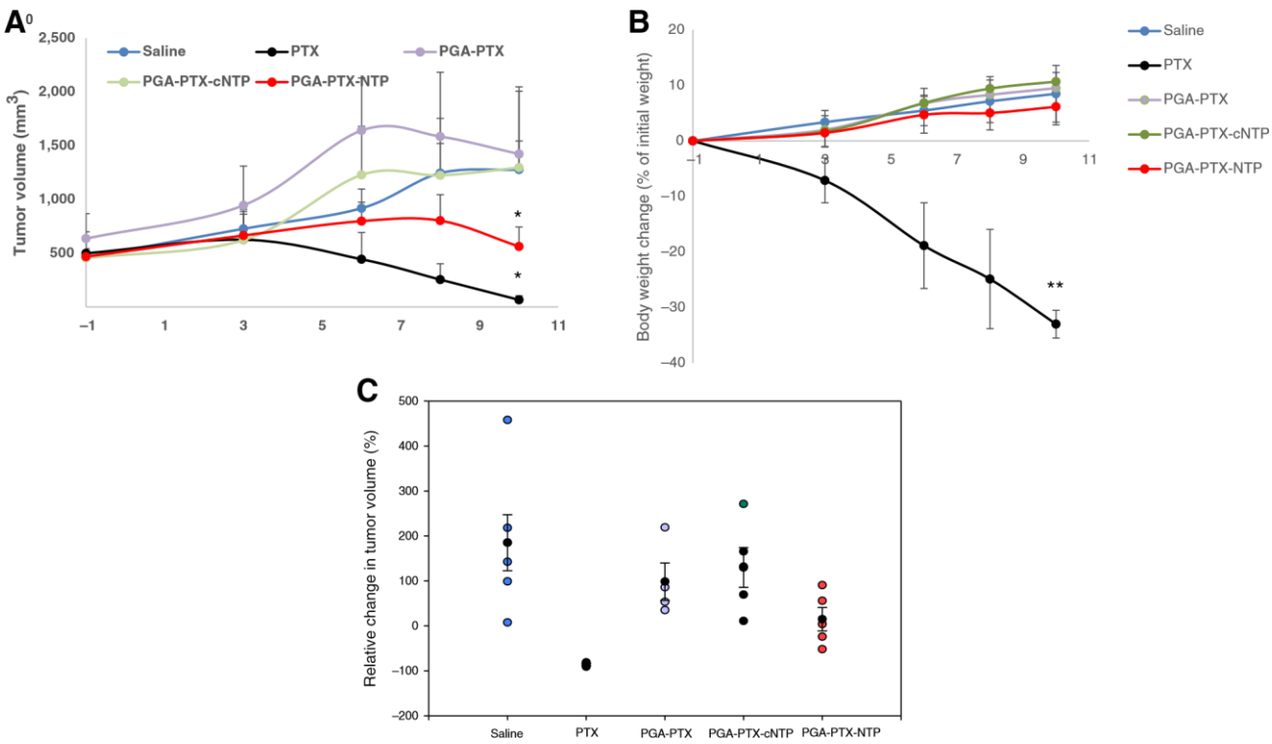

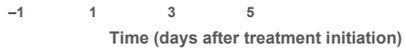

Figure 5.
Antitumor activity (A), toxicity (B) of PGA–PTX–NTP conjugate in WT model, and relative tumor volume compared with initial volume (C). Conjugates were administered at a concentration of 15 mg/kg PTX equivalent per treatment, every other day, for a total of five treatments, starting 4 weeks after tumor cell inoculation. Weight of the mice and tumor volume was monitored every other day. PGA–PTX–NTP conjugate inhibited tumor volume growth more than the control PGA–PTX–cNTP conjugate and the nontargeted PGA–PTX conjugate. Free PTX exhibited higher tumor growth inhibition; however, mice in the PTX-treated group suffered from toxic side effects and significant weight loss following treatments. , P< 0.05; , P< 0.01 PGA–PTX–NTP and PTX compared with saline, respectively, and , P< 0.05 PGA–PTX–NTP compared with PTX.

structures. They also demonstrated that NCAM was constitutively expressed by tumor-derived endothelial cells but not by normal endothelial cells (52). These results suggest that an NCAM-targeting conjugate can have a dual effect by inhibiting both the proliferation of tumor cells and formation of tumor vasculature. Indeed, we have found that the PGA–PTX–NTP conjugate effectively inhibited the organization of HUVEC into capillary-like tubes (36). These findings are relevant to WT as demonstrated here.

Targeting CSCs in WT was shown to have a great potential by using humanized anti-NCAM antibody–drug conjugate huN901DM1 (lorvotuzumab mertansine; ref. 17). In these experiments, huN901-DM1 inhibited the in vitro stemness properties of WT cell cultures that varied in the extent of NCAM expression. Furthermore, its in vivo targeting of multiple WT xenograft models was highly effective: WT bearing high NCAM expression, where NCAM population was enriched by passaging the tumors repeatedly in vivo, were completely or significantly eradicated. These results demonstrated the potential of targeting NCAM in a population of cells fueling the tumor and suggested that it can be a key target in appropriate developmental cancers bearing a primitive undifferentiated NCAMᵖ "blastema" phenotype. Indeed, we hypothesized that eradication by targeting the NCAMᵖ blastema, especially if >98% positive, would change the histologic appearance of the xenografts. However, the PGA–PTX–NTP treated tumors still appear to have predominantly blastema (small round blue cells) and with minimal stroma and no obvious or very few epithelia (Fig. 6) as seen by PAX8 staining. The explanation for this phenomenon might be that eradication of NCAMᵖ blastema WT CSCs allows selection of a more committed blastemal cell that is NCAM and lacks differentiation capacity to give rise to epithelial and stromal structure. In fact, it seems like the distribution of NCAMᵖ cells is such that they reside principally in the center of xenografts as can be seen in the saline-treated group (Fig. 6), and that after treatment with PGA–PTX–NTP, all that remains are the more peripheral NCAM cells that compress and comprise the surviving lesion. Moreover, PGA–PTX treatment resulted in apoptosis displayed only at peripheral margins, although we expected it to have a global effect. It seems that PGA–PTX follows recruited murine blood vessels, while the PGA–PTX–NTP effect occurred mainly in the center of xenografts supporting the cell specificity of the targeted strategy. These findings suggest that future studies should include treatments for a longer time period and an alternate dosing schedule.

Moreover, xenografts used in the in vivo experiments were blastema predominant and contained a minimal number of premature tubules (as seen in Fig. 6). Following the PGA–PTX– NTP treatment, we observed a change in the histological appearance of the xenografts that includes the disappearance of differentiated elements (from which NCAM expression is absent).

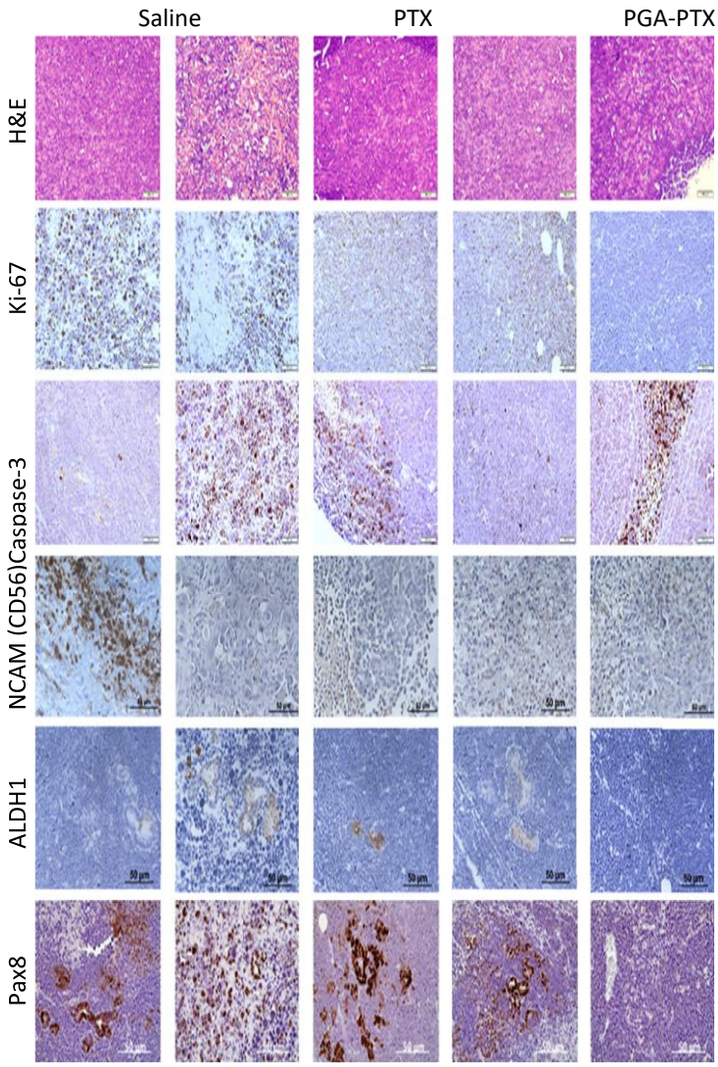

Figure 6.
Hematoxylin and eosin (H&E) staining of tumors show similar histology characteristics in the different treated g
Ki-67 staining shows complete absence of proliferation in PGA–PTX–NTP treated tumors, while in all other trea
staining shows extensive apoptosis in tumors treated with free PTX, PGA–PTX–NTP and PGA–PTX. In tumors tr
tumors, while in PGA–PTX treated tumors apoptosis is only seen at the margins. NCAM (CD56) staining was posi
positive in sections from PGA–PTX and PGA–PTX–cNTP and negative in sections from PGA–PTX– NTP treatmer
resulting in negative NCAM staining. ALDH1 staining showed positive staining in all groups except PGA–PTX–
PTX–NTP. Scale bars, 50 mm; objective, 400.

Thus, targeting the NCAMᵖ population may not eradicate all blastema, but elimination of the CSCs is likely to result in the disappearance of differentiated epithelial elements that are derivatives of the WT CSCs (15, 17, 18, 24). Previous results have indicated that differentiated elements within the blastema arise from the NCAMᵖ WT-CSC population. This population fuels the propagation of WT (15, 17, 18, 24); therefore, targeting NCAMᵖ WT-CSC depletes the tumor of these structures as can be seen in Fig. 6 (right, treatment with PGA–PTX–NTP). This suggests that anti-NCAM therapy should be implemented alongside other modalities so as to afford complete eradication of all tumor compartments. In fact, lorvotuzomab mertansine is currently under trial for relapsing WT

(https://clinicaltrials.gov/ct2/show/ NCT02452554). Importantly, NCAM is variably expressed as
different isoforms and with extensive posttranslational modifications, and these factors may influence antibody–drug conjugate binding and/or internalization. Thus, even if a valid therapeutic target such as NCAM exists, the target molecule may not be ideal from a clinical perspective. Accordingly, additional compounds should be developed and introduced to overcome the dependency on antibody specificity. PGA–PTX–NTP conjugate represents an attractive alternative as its binding to NCAM is dependent on a peptide and not an antibody, and is therefore less sensitive to posttranslational modifications.

In conclusion, our conjugate was highly effective in inhibiting proliferation and migration of xenograft-derived WT cells. Most importantly, the NCAM-targeted conjugate caused a reduction in tumor size in a patient-derived WT model and dramatically reduced the NCAM-expressing cell fraction, which was previously established as containing the CSC fraction of the tumor (12, 17). These results demonstrate that the PGA–PTX–NTP conjugate can be an effective tool to target and eradicate CSCs that are characterized by NCAM. Moreover, the activity seen on W011 cells is promising as this WT sample was originated from a recurrent disease, highlighting the PGA–PTX–NTP ability to target a treatment-resistant population of cells underscoring its therapeutic effect.

Disclosure of Potential Conflicts of Interest

No potential conflicts of interest were disclosed.

Authors' Contributions

Conception and design: E. Markovsky, E. Vax, O. Harari-Steinberg, N. Pode-Shakked, B. Dekel, R. Satchi-Fainaro

Development of methodology: E. Markovsky, E. Vax, I. Barshack, N. Pode-Shakked, R. Satchi-Fainaro

Acquisition of data (provided animals, acquired and managed patients, provided facilities, etc.): E. Markovsky, E. Vax, A. Eldar-Boock, E. Yeini, I. Barshack, R. Caspi

Analysis and interpretation of data (e.g., statistical analysis, biostatistics, computational analysis): E. Markovsky, E. Vax, D. Ben-Shushan, A. Eldar-Boock, R. Shukrun, I. Barshack, O. Harari-Steinberg, R. Satchi-Fainaro

Writing, review, and/or revision of the manuscript: E. Markovsky, E. Vax, D. Ben-Shushan, A. Eldar-Boock, E. Yeini, I. Barshack, B. Dekel, R. Satchi-Fainaro

Administrative, technical, or material support (i.e., reporting or organizing data, constructing databases): E. Vax, D. Ben-Shushan, E. Yeini, R. Caspi, R. Satchi-Fainaro

Study supervision: B. Dekel, R. Satchi-Fainaro

Acknowledgments

We thank Dr. Camila Avivi and Liat Anafi for their professional assistance with the histology staining and Dr. Hana Golan for her contribution to this study. E.M. thanks Tel Aviv University Center for Nanoscience and Nanotechnology for an excellence doctoral fellowship.

Grant Support

R. Satchi-Fainaro is supported by The Israel Science Foundation (grant no. 918/14), The European Research Council (ERC) Consolidator Award (617445, PolyDorm). B. Dekel is supported by The Ziering Foundation, The Israel Cancer Association (grant no. 20150916), The Israel Cancer Research Fund (ICRF) project grant (grant no. PG14112). This study was partially supported by the Tel-Aviv University, Sheba Medical Center Collaboration grant, the Israel Science Foundation (Grant No. 918/14), The European Research Council (ERC) Consolidator Award (617445, PolyDorm), and by grants from the Israeli National Nanotechnology Initiative (INNI), The Leona M. and Harry B. Helmsley Nanotechnology Research Fund and by Focal Technology Area (FTA) program: Nanomedicine for Personalized Theranostics.

The costs of publication of this article were defrayed in part by the payment of page charges. This article must therefore be hereby marked advertisement in accordance with 18 U.S.C. Section 1734 solely to indicate this fact.

Received March 1, 2017; revised June 14, 2017; accepted July 13, 2017; published OnlineFirst July 20, 2017.

References

1. Zecchini S, Cavallaro U. Neural cell adhesion molecule in cancer: expression and mechanisms. Neurochem Res 2008. doi:10.1007/s11064-0089597-9.
2. Bourne SP, Patel K, Walsh F, Popham CJ, Coakham HB, Kemshead JT. A monoclonal antibody (ERIC-1), raised against retinoblastoma, that recognizes the neural cell adhesion molecule (NCAM) expressed on brain and tumours arising from the neuroectoderm. J Neurooncol 1991;10:111–9.
3. Wachowiak R, Rawnaq T, Metzger R, Quaas A, Fiegel H, Kahler N, et al. Universal expression of cell adhesion molecule NCAM in neuroblastoma in contrast to L1: implications for different roles in tumor biology of neuroblastoma? Pediatr Surg Int 2008;24:1361–4.
4. Campodonico PB, de Kier Joffe ED, Urtreger AJ, Lauria LS, Lastiri JM, Puricelli LI, et al. The neural cell adhesion molecule is involved in the metastatic capacity in a murine model of lung cancer. Mol Carcinog 2010; 49:386–97.
5. Daniel L, Bouvier C, Chetaille B, Gouvernet J, Luccioni A, Rossi D, et al. Neural cell adhesion molecule expression in renal cell carcinomas: relation to metastatic behavior. Hum Pathol 2003;34:528–32.
6. Lantuejoul S, Laverriere MH, Sturm N, Moro D, Frey G, Brambilla C, et al. NCAM (neural cell adhesion molecules) expression in malignant mesotheliomas. Hum Pathol 2000;31:415–21.
7. Michalides R, Kwa B, Springall D, van Zandwijk N, Koopman J, Hilkens J, et al. NCAM and lung cancer. Int J Cancer Suppl 1994;8:34–7.
8. Winter C, Pawel B, Seiser E, Zhao H, Raabe E, Wang Q, et al. Neural cell adhesion molecule (NCAM) isoform expression is associated with neuroblastoma differentiation status. Pediatr Blood Cancer 2008;51:10–6.
9. Beckwith JB, Palmer NF. Histopathology and prognosis of Wilms tumors: results from the first national Wilms' tumor study. Cancer 1978;41: 1937–48.
10. Brok J, Treger TD, Gooskens SL, van den Heuvel-Eibrink MM, PritchardJones K. Biology and treatment of renal tumours in childhood. Eur J Cancer 2016;68:179–95.
11. Dekel B, Metsuyanim S, Schmidt-Ott KM, Fridman E, Jacob-Hirsch J, Simon A, et al. Multiple imprinted and stemness genes provide a link between normal and tumor progenitor cells of the developing human kidney. Cancer research 2006;66:6040–9.
12. Pode-Shakked N, Metsuyanim S, Rom-Gross E, Mor Y, Fridman E, Goldstein I, et al. Developmental Tumorigenesis: NCAM as a putative marker for the malignant renal stem/progenitor cell population. J Cell Mol Med 2008;13:1792–808.
13. Pode-Shakked N, Harari-Steinberg O, Haberman-Ziv Y, Rom-Gross E, Bahar S, Omer D, et al. Resistance or sensitivity of Wilms' tumor to anti-FZD7 antibody highlights the Wnt pathway as a possible therapeutic target. Oncogene 2011;30:1664–80.
14. Shukrun R, Pode Shakked N, Dekel B. Targeted therapy aimed at cancer stem cells: Wilms' tumor as an example. Pediatric nephrology (Berlin, Germany) 2013;29:815–23; quiz 21.
15. Pode-Shakked N, Pleniceanu O, Gershon R, Shukrun R, Kanter I, Bucris E, et al. Dissecting stages of human kidney development and tumorigenesis with surface markers affords simple prospective purification of nephron stem cells. Scientific Reports 2016;6:23562.
16. Rivera MN, Haber DA. Wilms' tumour: connecting tumorigenesis and organ development in the kidney. Nat Rev Cancer 2005;5:699–712.
17. Pode-Shakked N, Shukrun R, Mark-Danieli M, Tsvetkov P, Bahar S, PriChen S, et al. The isolation and characterization of renal cancer initiating cells from

human Wilms' tumour xenografts unveils new therapeutic targets. Embo Mol Med 2013;5:18–37.
18. Pode-Shakked N, Gershon R, Tam G, Omer D, Gnatek Y, Kanter I, et al. Evidence of in vitro preservation of human nephrogenesis at the single cell level. Stem Cell Reports 2017;in press.
19. Urbach A, Yermalovich A, Zhang J, Spina CS, Zhu H, Perez-Atayde AR, et al. Lin28 sustains early renal progenitors and induces Wilms tumor. Genes Dev 2014;28:971–82.
20. Hu Q, Gao F, Tian W, Ruteshouser EC, Wang Y, Lazar A, et al. Wt1 ablation and Igf2 upregulation in mice result in Wilms tumors with elevated ERK1/2 phosphorylation. J Clin Invest. 2011;121:174–83.
21. Pode-Shakked N, Dekel B. Wilms tumor–a renal stem cell malignancy? Pediatr Nephrol 2011;26:1535–43.
22. Reya T, Morrison SJ, Clarke MF, Weissman IL. Stem cells, cancer, and cancer stem cells. Nature 2001;414:105–11.
23. Dean M, Fojo T, Bates S. Tumour stem cells and drug resistance. Nat Rev Cancer 2005;5:275–84.
24. Shukrun R, Pode-Shakked N, Pleniceanu O, Omer D, Vax E, Peer E, et al. Wilms' tumor blastemal stem cells dedifferentiate to propagate the tumor bulk. Stem Cell Reports 2014;3:24–33.
25. Wood AC, Maris JM, Gorlick R, Kolb EA, Keir ST, Reynolds CP, et al. Initial testing (stage 1) of the antibody-maytansinoid conjugate, IMGN901 (Lorvotuzumab mertansine), by the pediatric preclinical testing program. Pediatr Blood Cancer 2013;60:1860–7.
26. Fiegel HC, Gluer S, Roth B, Rischewski J, von Schweinitz D, Ure B, et al. Stem-like cells in human hepatoblastoma. J Histochem Cytochem 2004;52:1495–501.
27. Xu X, Xing B, Han H, Zhao W, Hu M, Xu Z, et al. The properties of tumorinitiating cells from a hepatocellular carcinoma patient's primary and recurrent tumor. Carcinogenesis 2009.
28. Buescher JM, Margaritis A. Microbial biosynthesis of polyglutamic acid biopolymer and applications in the biopharmaceutical, biomedical and food industries. Crit Rev Biotechnol 2007;27:1–19.
29. Eldar-Boock A, Miller K, Sanchis J, Lupu R, Vicent MJ, Satchi-Fainaro R. Integrin-assisted drug delivery of nano-scaled polymer therapeutics bearing paclitaxel. Biomaterials 2011;32:3862–74.
30. Li C. Poly(L-glutamic acid)–anticancer drug conjugates. Adv Drug Deliv Rev 2002;54:695–713.
31. Strojnik T, Zajc I, Bervar A, Zidanik B, Golouh R, Kos J, et al. Cathepsin B and its inhibitor stefin A in brain tumors. Pflugers Arch 2000;439: R122–3.
32. Strojnik T, Kos J, Zidanik B, Golouh R, Lah T. Cathepsin B immunohistochemical staining in tumor and endothelial cells is a new prognostic factor for survival in patients with brain tumors. Clin Cancer Res 1999;5:559–67.
33. Decock J, Obermajer N, Vozelj S, Hendrickx W, Paridaens R, Kos J. Cathepsin B, cathepsin H, cathepsin X and cystatin C in sera of patients with early-stage and inflammatory breast cancer. Int J Biol Markers 2008;23:161–8.
34. Foekens JA, Kos J, Peters HA, Krasovec M, Look MP, Cimerman N, et al. Prognostic significance of cathepsins B and L in primary human breast cancer. J Clin Oncol 1998;16:1013–21.
35. Markovsky E, Baabur-Cohen H, Satchi-Fainaro R. Anticancer polymeric nanomedicine bearing synergistic drug combination is superior to a mixture of individually-conjugated drugs. J Control Rel 2014;187: 145–57.
36. Markovsky E, Eldar-Boock A, Ben-Shushan D, Baabur-Cohen H, Yeini E, Pisarevsky E, et al. Targeting NCAM-expressing neuroblastoma with polymeric precision nanomedicine. J Control Rel 2017;249:162–72.
37. Ramanathan RK, Rubin JT, Ohori NP, Belani CP. Dramatic response of adult wilms tumor to paclitaxel and cisplatin. Med Pediatr Oncol 2000;34:296–8.
38. Ozaki S, Takigawa N, Ichihara E, Hotta K, Oze I, Kurimoto E, et al. Favorable response of heavily treated Wilms' tumor to paclitaxel and carboplatin. Onkologie 2012;35:283–6.
39. Morabito V, Guglielmo N, Melandro F, Mazzesi G, Alesini F, Bosco S, et al. Adult Wilms tumor: case report. Int J Surg Case Rep 2015;6C:273–6.
40. Ronn LC, Olsen M, Ostergaard S, Kiselyov V, Berezin V, Mortensen MT, et al. Identification of a neuritogenic ligand of the neural cell adhesion molecule using a combinatorial library of synthetic peptides. Nat Biotechnol 1999;17:1000–5.
41. Popov SD, Sebire NJ, Vujanic GM. Wilms' tumour - histology and differential diagnosis. In: van den Heuvel-Eibrink MM, editor. Wilms Tumor. Brisbane (AU)2016.
42. Jensen M, Berthold F. Targeting the neural cell adhesion molecule in cancer. Cancer Lett 2007;258:9–21.
43. Klehr M, Muehlenhoff M, Berthold F, Jensen M. Humanized antibodies against the neural cell adhesion molecule (NCAM) as a new approach to the targeting of neuroblastoma. Klin Padiatr 2006;218:189-.
44. Roguska MA, Pedersen JT, Keddy CA, Henry AH, SearleSJ, Lambert JM, et al. Humanization of murine monoclonal antibodies through variable domain resurfacing. Proc Nat Acad Sci USA 1994;91:969–73.
45. Whittington HA, Hancock J, Kemshead JT. Generation of a humanised single chain Fv (Scfv) derived from the monoclonal Eric-1 recognising the human neural cell adhesion molecule. Med Pediatric Oncol 2001;36: 243–6.
46. Chanan-Khan AA, Jagannath S, Munshi NC, Schlossman RL, Anderson KC, Lee K, et al. Phase I study of huN901-DM1 (BB-10901) in patients with relapsed and relapsed/refractory CD56-positive multiple myeloma. Blood 2007;110:356a–a.
47. Chari RVJ, Derr SM, Ferris CA, Steeves RM, Widdison WC. HuN901-DM1: a tumor-activated prodrug that eradicates large xenografts of small cell lung cancer in mice and shows minimal toxicity in cynomolgus monkeys. Clinical Cancer Research 1999;5:3822s–s.
48. Chari RVJ, Steeves RM, Xie HS, Widdison WC, Lambert JM. Preclinical development of huN901-DM1: a tumor-activated prodrug directed against small cell lung cancer. Clinical Cancer Research 2000;6:4489s–s.
49. Fidias P, Grossbard M, Lynch TJ Jr.A phase II study of the immunotoxin N901-blocked ricin in small-cell lung cancer. Clin Lung Cancer 2002; 3:219–22.
50. Hopkins K, Chandler C, Eatough J, Moss T, Kemshead JT. Direct injection of 90Y MoAbs into glioma tumor resection cavities leads to limited diffusion of the radioimmunoconjugates into normal brain parenchyma: a model to estimate absorbed radiation dose. Int J Rad Oncol Biol Phys 1998;40: 835–44.
51. Ishitsuka K, Jimi S, Goldmacher VS, AbO, Tamura K.Targeting CD56 bythe maytansinoid immunoconjugate IMGN901 (huN901-DM1): a potential therapeutic modality implication against natural killer/T cell malignancy. Brit J Haematol 2008;141:129–31.
52. Bussolati B, Grange C, Bruno S, Buttiglieri S, Deregibus MC, Tei L, et al. Neural-cell adhesion molecule (NCAM) expression by immature and tumor-derived endothelial cells favors cell organization into capillary-like structures. Exp Cell Res 2006;312:913–24.